Journal of Physics and Its Applications

Journal homepage : https://ejournal2.undip.ac.id/index.php/jpa/index

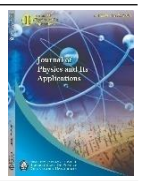

Analytical Solution in the (*I-V*) Characteristic Curves Calculation of the Corona Plasma Discharge Using the Capacitance Model

Asep Yoyo Wardaya[1*], Zaenul Muhlisin[1], Jatmiko Endro Suseno[1], Evi Setiawati[1], Susilo Hadi[2], Mustati'ah[1], and Jaka Windarta[3]

[1]*Department of Physics, Faculty of Science and Mathematics, Diponegoro University, Semarang, Indonesia*
[2]*Department Physique, Université de Rouen Normandie, Avenue De L'universite 76801 St Et. Du Rouvray Cedex, France*
[3]*Department of Electrical Engineering, Faculty of Engineering, Diponegoro University, Semarang, Indonesia*

**Corresponding author:asepyoyowardayafisika@gmail.com*

A R T I C L E I N F O

Article history:
Received: 8 December 2024
Accepted: 30 July 2025
Available online: 31 August 2025

Keywords:
Corona discharge
The curve of (I-V) characteristics
TTDA-P
Multiplying factor k
Python GUI program

A B S T R A C T

This research aims to calculate thoroughness among data points and analytical simulation curves in discussing corona discharges' (I-V) characteristics. The electrode construction used is the twin towers with dividing angles to the plane (TTDA-P) model in air, with negative DC polarity. An asymmetrical electrical CCP model in the electrode design uses research variations, including active electrode center clamp angles of θ = 30^0, 45^0, and 60^0 and active and passive electrode distances (d) of 0.002 m, 0.005 m, and 0.008 m. The simulation curve comes from the analytical formulation of the reduced capacitance type (inserting a multiplying factor k to the sharp corners of the active electrode), with the simulation program being a Python GUI program. The experimental results produced an appropriate error value (t-test value ≤0.05) and a high percentage of tangent points value. The best curve was achieved at θ = 45^0 and d = 0.008 m, with a t-test value of 0.0313 and the highest percentage of significant tangent points of 92.31%. For all variations θ, there is a tendency that the smaller the value of d (the gap length among two electrodes), the greater the deviation distance between the simulation curve and the data points.

1. Introduction

Plasma discharge technology has developed rapidly in various research fields, including medical physics [1], agriculture and biomedicine [2], fusion plasma [3], Etc. Some equipment from plasma technology is analogous to capacitor equipment, named capacitively coupled plasma (CCP) [4]. The CCP equipment has three categories: the electric asymmetric CCP, the direct current CCP, and the dual-frequency CCP [5]. The CCP model categories in this research are asymmetric electric and direct current with negative corona discharge polarity. Calculating current-voltage (*I-V*) characteristics in electrical circuits using capacitors or other conventional electrical equipment differs from electrical circuits in CCP equipment. There are various (*I-V*) characteristic forms that are unique to CCP equipment caused by several physical events such as Electrohydrodynamic (EHD) flow [6], convective heat transfer [7], electric wind [8], electrostatic precipitation [9], etc., resulting in analytical solutions with a reasonably high level of difficulty, compared to the analytical solution of the (*I-V*) characteristics produced by a conventional electrical circuit (not the case of plasma discharge).

Although the (*I-V*) characteristics of plasma discharges are caused by various physical properties, in the Robinson's paper [10], there is an approach to model the (*I-V*) characteristics of plasma discharges for the case of coaxial cylinders through the following formulation,

$$i = \frac{I}{l} = \frac{10^6}{l}\frac{4b_0 C_{CC}}{\sigma R^2} V\left(V - V_i\right), \tag{1}$$

where I is corona current (A), i is corona current/length (A/m), and σ is the density of the air relative to standard conditions (250C, 76 cm Hg) in the range of $0.1 < \sigma < 35$. The quantities R and l are the radii of the outer cylinder and the length of the Coaxial Cylinders, respectively. The C_{CC} quantity is a capacitance formulation of a cylindrical coaxial electrode shape [11] that is,

$$C_{CC} = \frac{2\pi\varepsilon l}{\ln\left(R/r\right)}, \tag{2}$$

where r is the radii of the inner cylinder (thin wire), by looking at the form of Eq. (1), we can conclude that the (*I-V*) characteristics of the plasma discharge depend on the value of the capacitance of the coaxial cylindrical shape, with the nature of the plasma flow being radially symmetric (there is an R^{-2} function) from the Eq. (1).

Other CCP models, such as an asymmetric electrode arrangement where the two electrodes are perpendicular (using a Cartesian coordinate system),

cannot use the radial symmetric concept as in Eq. (1). Wardaya et al. [12, 13] have introduced a (*I-V*) characteristic solution model for the asymmetric CCPs case by adding a corona current multiplying factor (referred to as factor *k*) at the integration limit of the sharpest area of the tip of the active electrode in the capacitance calculation (the reduced capacitance model/RCM). This model is proven adequate and similar in concept to the corona current multiplier factor of 10^6 in Eq. (1). However, the multiplier factor in the case of asymmetric CCP only appears at the sharpest tip of the active electrode, as shown by the experiments of Dobranszky et al. [14], where the corona current will be visible coming out of the sharp edges of the active electrode.

This research aims to calculate the level of match between the analytical formulation and research data on the (*I-V*) characteristic equation with the CCP electrode construction model, namely Twin towers with dividing angles to the plane (TTDA-P) at negative dc polarity. The (*I-V*) Characteristic curves, which include analytical curves and experimental data points, are processed through Python GUI Programming. This program will also determine the k factor's value (functions as a curve fitting) and graphical corrections such as standard deviation (*SD*) and t-test values. This research is essential in the development of science because it reveals several new contributions. One of them is the use of a new research method using the geometric properties of asymmetric CCP equipment, as reflected in the appearance of the factor *k* on the sharp part of the active electrode tip in capacitance calculations. This approach differs from the research method using the physical properties of plasma through calculations based on Maxwell's equations. In addition, the analytical formulation of the current versus voltage function involves variations in the size of the CCP equipment, which includes the distance between electrodes *d* and the center clamp angle (θ).

The benefit of this research is introducing a new analytical calculation method that can be used to measure the (*I-V*) characteristics from the equipment of the electric asymmetric CCP used by the wider community.

2. Methods

The electrode construction model (TTDA-P) consists of two electrodes in air, with the active electrode positioned asymmetrically above the passive electrode, with the gap length between the two electrodes of *d*, as shown in Fig. 1. The two electrodes are in the place of perpendicular to each other. The active electrode is made of thin copper with a shape like an arrangement of rectangular and twin triangular plates. The θ-angle gap (center clamp angle) is in the middle of the twin triangular. Meanwhile, the passive electrode (also made of copper) has a reasonably large area and can accommodate all the current flow that came out of the active electrode. The active electrode thickness is δ = (0.00012 ± 0.00001) m and has length and width dimensions of *a* = 0.02 m and *b* = 0.045 m. The research variations used include angle variations θ of 30^0, 45^0, and 60^0 and distance variations *d* of 0.002 m, 0.005 m, and 0.008 m.

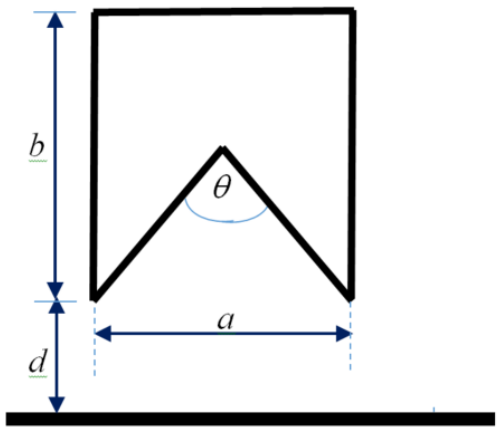

Fig. 1: Illustration of the TTDA-P electrode construction model

The illustration of the negative DC polarity electrical circuit of the plasma discharge in this research in Fig. 2,

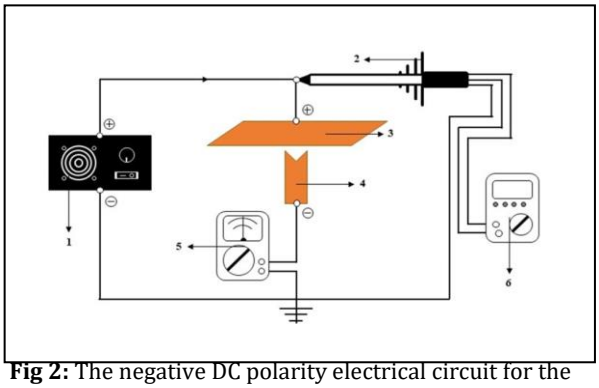

Fig 2: The negative DC polarity electrical circuit for the TTDA-P construction model

Fig. 2 illustrates the negative DC polarity electrical circuit for the TTDA-P electrode construction model. A high-voltage probe, capable of converting voltage from kV to V with a maximum DC capacity of 40 kV, is connected to the system. The passive electrode is also made of rectangular copper metal but designed in the twin towers with dividing angles (TTDA) form. The circuit also includes an Ampere meter with specifications of Vmax AC 750 V and DC 1000 V, using the SANWA type CX506a brand, as well as a SANWA CD771 brand voltmeter for voltage measurement.

In this experiment, the positive or negative value of a corona discharge is determined by the polarity of the voltage or the arrangement of the electrodes, which have sharp surfaces. A DC negative corona discharge is caused by the negative voltage pole connected to the active electrode (which has a sharp surface shape) [15]. This research uses an electrode arrangement of CCP equipment with a DC voltage source for a negative corona discharge polarity case. In the corona discharge case, the calculation of the current-voltage (*I-V*) characteristics usually uses the following equation [8, 12, 16, 17],

$$I = C_k \left(V - V_i\right)^2 \quad \text{or} \quad I = C_k \; V\left(V - V_i\right), \qquad (3)$$

where I is the corona current, V is the applied voltage, V_i is the apparent corona-starting voltage, and C_k is a specific constant defined as a geometric function [8].

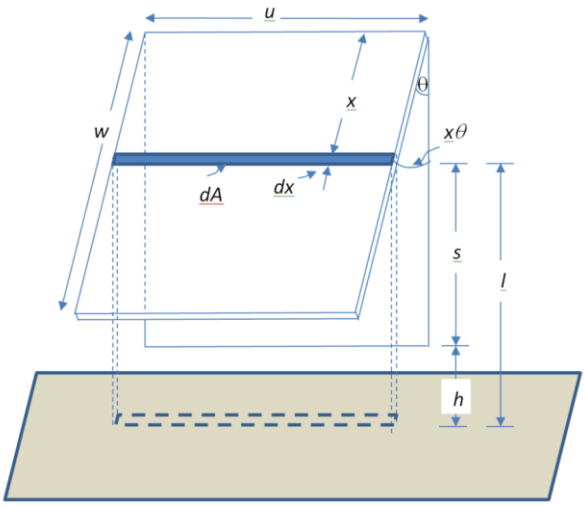

Fig. 3: The depiction of the arrangement of the electrodes for the knife-to-plane construction model

If we compare Eq. (1) and (3), we conclude that the quantity C_k is a capacitance function. Calculation of capacitance (at quantity C_k) from the (TTDA-P) electrode construction model uses the concept of reduced capacitance model (RCM) [13]. There is another model reference as a basis for RCM calculations in this research, called the knife-to-plane construction model, expressed in Fig. 3. In the figure, there is an arrangement of active and passive electrodes, with the passive electrode having a length and width of u and w, respectively, with the active electrode position being tilted to the vertical plane by θ. The gap length between the active electrode (at a minimal angle θ) and the passive electrode (lying below the active electrode) is h. The active electrode has an element of area dA with length u and width dx and a distance of $l = h + s$ from the passive electrode.

For the case when the active electrode position is perpendicular to the passive electrode position ($\theta \cong 0$), the relationship $s = w - x$ is obtained, and the capacitance element value (from the area element dA) is obtained as

$$dC = \varepsilon_0 \frac{dA}{l} = \varepsilon_0 \frac{u\,dx}{h + w - x}. \qquad (4)$$

The calculation of the capacitance element in Eq. (4) is obtained from the capacitance value formulation for the parallel plate case of $C = \varepsilon_0 A/l$ [11]. The solution to Eq. (4) is the capacitance value of the knife-to-plane electrode construction model, which is written as,

$$C_{lp} = -\varepsilon_0 u \int_{x=0}^{w} d \ln|x - h - w| = \varepsilon_0 u \ln\left|\frac{h+w}{h}\right|. \qquad (5)$$

From Fig.1, we assume that the active electrode of the TTDA-P construction model consists of four-sided and twin-triangular plates. Calculating the RCM function for all plate parts uses the primary reference of the C_{lp} value in Eq. (5). For the four-sided plate part of the active electrode (illustrated in Fig. 4), the similar formulation as electrode construction model of the knife-to-plane in eq. (5), with the value of the capacitance, is

$$C_{4\text{-sided}} = \varepsilon_0\, a \ln\left|\frac{b+d}{\frac{1}{2}a\cot\left(\frac{1}{2}\theta\right)+d}\right|, \qquad (6)$$

with the variables relationship between Eq. (5) and Eq. (6) is,

$$u = a \;;\; w = b - \tfrac{1}{2}a\cot\left(\tfrac{1}{2}\theta\right) \;;\; h = d + \tfrac{1}{2}a\cot\left(\tfrac{1}{2}\theta\right) \quad (7)$$

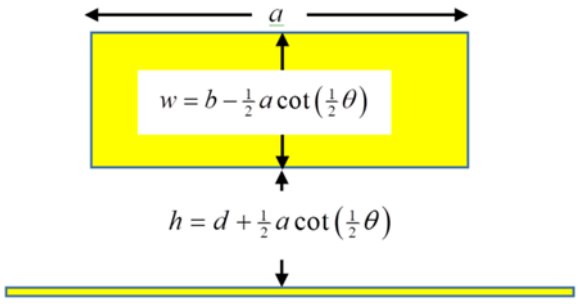

Fig. 4: The four-sided plate of the active electrode in the TTDA-P construction model

Calculate the RCM function for the case of twin triangular active electrodes using capacitance elements. This concept starts from calculating the rectangular area element from the capacitance calculation in Eq. (5). Now consider Fig. 5, which depicts the shape of a twin triangular plate with the u-axis and v-axis for the horizontal and vertical axes, respectively. The v-axis divides the twin triangular plates symmetrically.

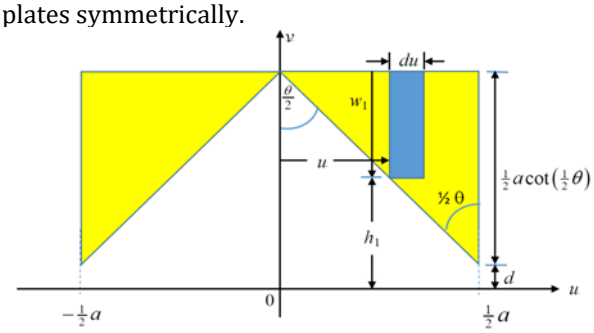

Fig. 5: The TTDA-P construction model for the twin-triangular plate shape (active electrode).

Because there is a symmetry characteristic, calculating the capacitance value on the active electrode part of the two plate twin triangles concerning the passive electrode, we only calculate the capacitance part to the right side of the v-axis coordinate so that the total capacitance in this case becomes

$$C_{tot\Delta} = 2C_{\Delta}. \qquad (8)$$

The C_Δ is the triangular plate's capacitance value located on the right side of the v-axis coordinate. Now, we can compare the capacitance value C_{lp} from Eq. (5) in Fig. 3 with the capacitance element value dC_Δ in Fig. 5. In the C_{lp} calculation, there are several variable quantities such as length u, width w, and the distance between the electrodes h, while in the dC_Δ calculation, there are several variable quantities such as length du, width w_1, and the distance between the active electrode elements and the passive electrode h_1. By paying attention to these proportional values, the capacitance element value in Fig. 5 is

$$dC_{\Delta} = \varepsilon_0\, du \ln\left|\frac{w_1 + h_1}{h_1}\right|, \qquad (9)$$

with the relationship of the variables in Eq. (9) to the variables contained in Fig. 5 through the following equations,

$$w_1 = u\cot\left(\tfrac{1}{2}\theta\right), \qquad h_1 + w_1 = d + \tfrac{1}{2}a\cot\left(\tfrac{1}{2}\theta\right), \quad 0 \le u \le \tfrac{1}{2}a, . \tag{10}$$

Let us look at a whole system TTDA-P model (Fig. 1) consisting of a four-sided plate and a twin-triangle plate. The location of the four-sided plate (Fig. 4) is above the part of the twin triangles plate (Fig. 5), so the relationship $h = h_1 + w_1$ applies. Furthermore, the total solution of the capacitance value originating from the twin triangles plate system through the relationship of Eq. (8) – (10) is

$$C_{tot\Delta} = 2\varepsilon_0 \int_{u=0}^{a/2} du \ln\left|\frac{d + \tfrac{1}{2}a\cot\left(\tfrac{1}{2}\theta\right)}{d + \tfrac{1}{2}a\cot\left(\tfrac{1}{2}\theta\right) - u\cot\left(\tfrac{1}{2}\theta\right)}\right|. \tag{11}$$

Eq. (11) is a capacitance solution suitable for the case of ordinary conventional circuits, which is not suitable for the case of corona discharge. Based on experiments of Dobranszky et al. [14], the corona discharge will be seen most significantly and brightest coming out of the sharp lower edges of the active electrode, which in this study is located at the position $u = \pm a/2$ in Fig. 5. Following research of Wardaya et al. [12, 13], the solution for the RCM concept is to add a current multiplying factor k to the integration limit at the point $u = \pm a/2$. Using the RCM concept in Eq. (11), then the capacitance formulation will be,

$$\left(C_{tot\Delta}\right) = 2\varepsilon_0 \int_{u=0}^{ka/2} du \ln\left|\frac{d + \tfrac{1}{2}a\cot\left(\tfrac{1}{2}\theta\right)}{d + \tfrac{1}{2}a\cot\left(\tfrac{1}{2}\theta\right) - u\cot\left(\tfrac{1}{2}\theta\right)}\right|. \tag{12}$$

Then, we get the solution of Eq. (12) as

$$\left(C_{tot\Delta}\right) = \left[2\varepsilon_0 d\tan\left(\tfrac{1}{2}\theta\right) + a\varepsilon_0 - ka\varepsilon_0\right]\ln\left|\frac{\tfrac{1}{2}ka\cot\left(\tfrac{1}{2}\theta\right) - d - \tfrac{1}{2}a\cot\left(\tfrac{1}{2}\theta\right)}{d + \tfrac{1}{2}a\cot\left(\tfrac{1}{2}\theta\right)}\right| + k\varepsilon_0 a\ . \tag{13}$$

By adding the solutions of Eqs. (6) and (13), we obtain the total solution of the capacitance equation for the TTDA-P electrode construction model as,

$$C_{tot} = C_{\text{rect}} + \left(C_{tot\Delta}\right) = \varepsilon_0\, a\ln\left|\frac{b+d}{\tfrac{1}{2}a\cot\left(\tfrac{1}{2}\theta\right) + d}\right| + k\varepsilon_0 a + \left[2\varepsilon_0 d\tan\left(\tfrac{1}{2}\theta\right) + a\varepsilon_0 - ka\varepsilon_0\right]\ln\left|\frac{\tfrac{1}{2}ka\cot\left(\tfrac{1}{2}\theta\right) - d - \tfrac{1}{2}a\cot\left(\tfrac{1}{2}\theta\right)}{d + \tfrac{1}{2}a\cot\left(\tfrac{1}{2}\theta\right)}\right| \tag{14}$$

At the bottom of the active electrode, there is a Gaussian area that flows plasma current consisting of the area around the length of line a and two sharp points at the bottom ends, with the formulation as

$$A = \delta a + 2\delta^2. \tag{15}$$

The thickness dimension of the active electrode plate is δ = (0.12 ± 0.01)×10^{-3} m. The complete formulation of electric current as a function of voltage for the TTDA-P electrode construction model using the relationship from Eq. (3) is [18]

$$I = -\frac{\mu_0\left(C_{tot}\right)^3\left(V - V_i\right)^2}{\varepsilon_0{}^2\left(\delta a + 2\delta^2\right)^2}, \tag{16}$$

where A is Gaussian surface area, ε_0 = 8.854×10^{-12} F m^{-1} and μ_0 = 4π×10^{-7} Hm^{-1} are vacuum permittivity and vacuum permeability, respectively. For conditions in the air at STP, there is a relationship ε = 1.00058986 ε_0 and μ = 1.00000037 μ_0, so the conditions $\mu_0 \cong \mu$ and $\varepsilon_0 \cong \varepsilon$ apply. Eq. (16) is the (*I-V*) characteristic equation of CCP equipment using the concept of the geometric function of the C_{tot} value in Eq. (14).

In this experiment, a simulation program uses Python GUI Programming to obtain a level of compatibility between analytical calculations and experimental data. The simulation curve from analytical calculations comes from the characteristic formulation (I-V) in Eq. (16), which already contains the geometric properties of the plasma discharge in the formulation of the C_{tot} capacitance value (using a multiplier factor k). In this case, the value k is a fitting curve graph. The Python GUI Programming will calculate the value k that matches the graph and, at the same time, also calculate the level of accuracy of the curve, which includes the values of standard deviation (SD), t-test, and tangent point programs.

The requirements for the simulation curve from ideal analytical calculations to be close to the experimental data values involve several aspects, such as having the value of the smallest t-test (maximum value of 0.05) [19], a small SD value and a significant percentage value of tangent points. In order to match the function, the Python GUI uses a second-rank polynomial form adopted from the formulation (16) based on the equation,

$$I = a_0 + a_1 V + a_2 V^2, \tag{17}$$

where a_0, a_1, and a_2 are constant valued quantities in the function of voltage V. Meanwhile, SD in this study uses the formulation [19].

$$\sigma = \sqrt{\frac{\sum_i \left(I - A_1 - A_2 V_i - A_3 V_i^2\right)^2}{(N-2)}}, \tag{18}$$

with the values A_1, A_2, and A_3 obtained through Eq. (19)

$$\begin{bmatrix} N & \sum V_i & \sum V_i^2 \\ \sum V_i & \sum V_i^2 & \sum V_i^3 \\ \sum V_i^2 & \sum V_i^3 & \sum V_i^4 \end{bmatrix}\begin{bmatrix} A_1 \\ A_2 \\ A_3 \end{bmatrix} = \begin{bmatrix} \sum I_i \\ \sum V_i I_i \\ \sum V_i^2 I_i \end{bmatrix}, \tag{19}$$

3. Result and discussion

Fig. 6 is the (*I-V*) characteristic curve of a corona discharge, which consists of a simulation curve for analytical calculations from Eq. (16) and data points from the function of electric current versus voltage. The active electrode of the TTDA-P construction model has the same size values at a = 0.02 m and b =0.045 m. This electrode has variations in the center clamp angle θ at 30^0, 45^0, and 60^0 angles. For each θ, three variations of d (the gap length between two electrodes) were made at sizes 0.002 m, 0.005 m, and 0.008 m, resulting in 9 variations of the (*I-V*) characteristic curve in Fig. 6.

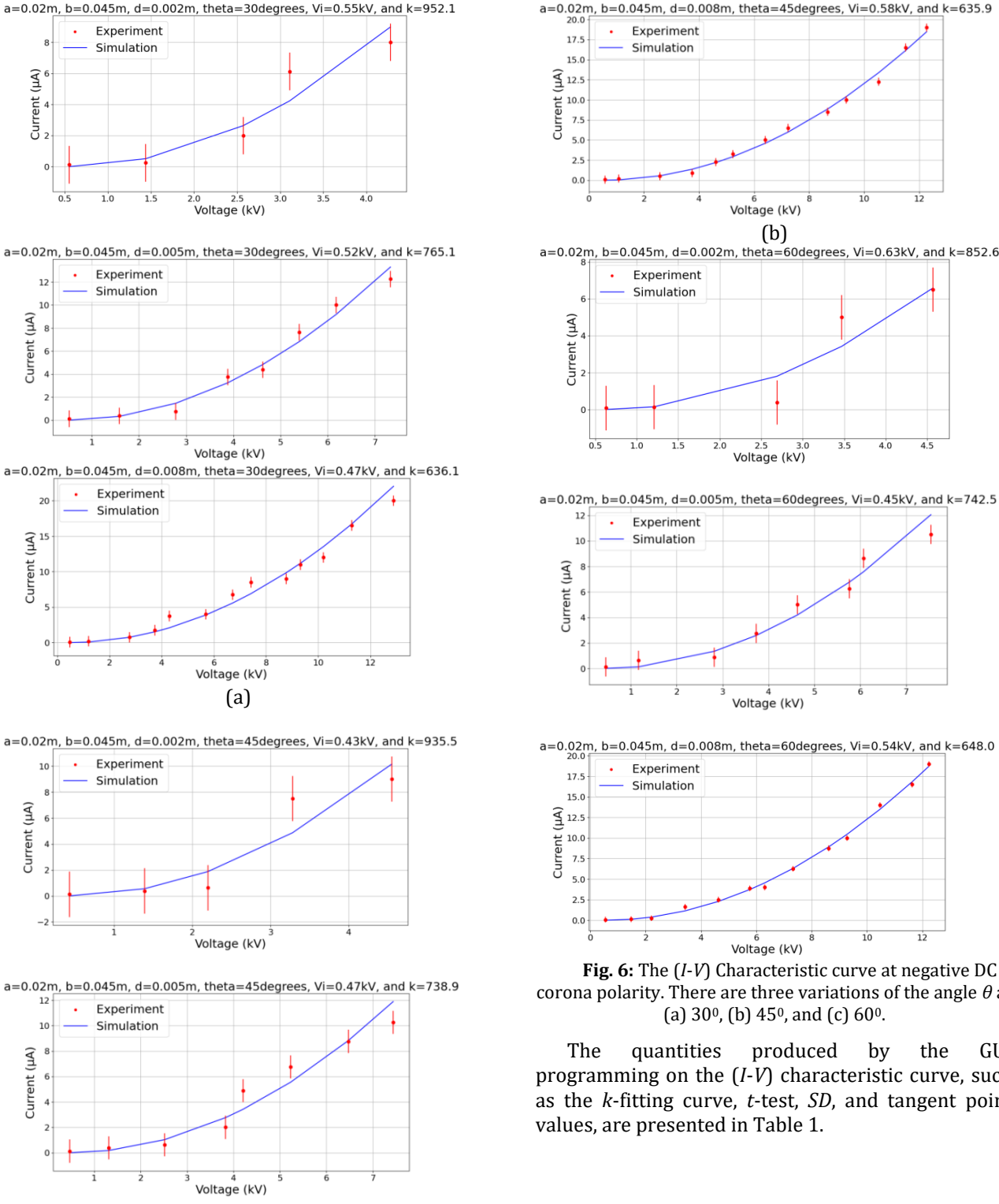

Fig. 6: The (*I-V*) Characteristic curve at negative DC corona polarity. There are three variations of the angle θ at (a) 30^0, (b) 45^0, and (c) 60^0.

The quantities produced by the GUI programming on the (*I-V*) characteristic curve, such as the *k*-fitting curve, *t*-test, *SD*, and tangent point values, are presented in Table 1.

Table 1 The quantities of the *k*-fitting curve, *t*-test, *SD*, and tangent point values of the (*I-V*) characteristic curve

θ	***d(m)***	***Vi*** *(kV)*	***t-test***	***SD*** *(μA)*	***Tangent Point***	***Percentage*** *(%)*	***k***
	0.002	0.55	0.0495	1.2097	4 of 5	80	952.1
30^o	0.005	0.52	0.0419	0.7215	5 of 8	62.5	765.1
	0.008	0.47	0.0394	0.7451	7 of 13	53.8	636.1
	0.002	0.43	0.0493	1.7496	4 of 5	80	935.5
45^o	0.005	0.47	0.0458	0.9103	5 of 8	62.5	738.9
	0.008	0.58	0.0313	0.4938	12 of 13	92.31	635.9
	0.002	0.63	0.0489	1.207	3 of 5	60	852.6
60^o	0.005	0.45	0.0468	0.7514	5 of 8	62.5	742.5
	0.008	0.54	0.0485	0.3352	9 of 13	69.23	648.0
average value			0.0446	0.903		69.204	

Fig. 7 shows experimental results in corona discharge photographs for the variations of three angle θ of the active electrode with the TTDA-P construction model.

(a)

(b)

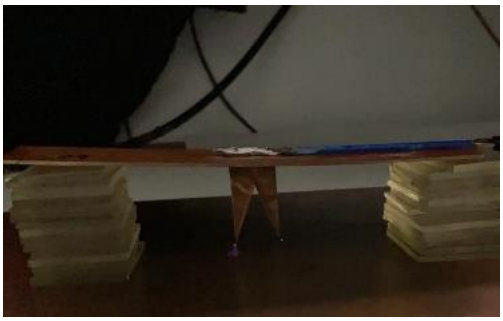

Fig. 7: The corona discharge photographs for variations of the three angle θ of a) 30^0, b) 45^0, and c) 60^0.

Now, we look again at Table 1, which provides an explanation of several experimental results. From the table, it can be seen that all t-test values are below 0.05. The lowest t-test value is 0.0313 (at an angle variation of $\theta = 45^0$ with a value of d = 0.008 m), producing the highest percentage of tangent points of 92.31%. The most significant t-test value is 0.0495 (at an angle variation of $\theta = 30^0$ with a value of d = 0.002 m) and produces a high percentage of tangent point of 80%. On average, the case of d = 0.002 m produces the bigger t-test and SD values (compared to the values d = 0.005 m and d = 0.008 m), while the minimum t-est and SD values in the varied case between d = 0.005 m and d = 0.008 m. The SD quantities have values that vary from small to large. The smallest SD value is 0.3352 (at an angle variation of $\theta = 60^0$ with a value of d = 0.008 m), while the most significant SD value is 1.7496 (at an angle variation of $\theta = 45^0$ with a value of d = 0.002 m). Overall, for all variation data θ and d in Table 1, it has a relatively high percentage of tangent point values.

The research results presented in Table 1 are discussed in relation to the (I-V) characteristic curve shown in Fig. 6. The t-test value <0.05 for all variations of θ and d, indicating a high level of accuracy between analytical calculations and research data. Suppose we examine Fig. 6 for the variation of the angle $\theta = 45^0$ and d = 0.008 m, which produces the lowest t-test value of 0.0313 (as shown in Table 1). In this case, it turns out to create a curve slope that best fits the data points compared to the overall characteristic curve (because the figure has the combined criteria of a relatively large percentage of tangent points and a small SD value that indicates the highest level of accuracy between analytical calculations and experimental data), so it is the best characteristic curve in Fig. 6. Meanwhile, Fig. 6, with the most significant t-test value of 0.0489 (in the variation of $\theta = 60^0$ and d = 0.002 m), turns out to produce a curve slope that is quite far from the range of data points (because it has the smallest number and percentage of tangent points and a considerable SD value). A smaller SD value indicates a high level of accuracy between the analytical calculation curve and the data points, as indicated by shorter vertical lines (SVL), specifically the red line, which contains a data point. At the same time, the high number and percentage of tangent points indicate a high rate of intersections between the analytical curve and the data points.

In general, for all angles $\theta = 30^0$, 45^0 and 60^0, the analytical curve will be closer to the value of the data points in the order of distance d = 0.002 m, 0.005 m, and 0.008 m, because it has an increasing number of tangent points (although the percentage sometimes decreases) with a decreasing SD value. Although at an angle $\theta = 30^0$, the SD value increases slightly (not too significantly) from d = 0.005 m to 0.008 m, so that the length of the SVL at both d values is almost the same (taking into account the different range of voltage and current coordinates in the two images).

The reason why the characteristic curve with d = 0.002 m has the smallest accuracy level (among the analytical curves with data points) compared to the characteristic curves at other distances d is that it has the most significant SD value, thus having the longest SVL size. Let's examine Eq. (18) and (19). The significant σ (SD) value arises from the contribution of the I value increasing too quickly compared to the voltage value V in the analytical calculation, as opposed to the position of the data points. For the calculation of coefficients A_1, A_2, and A_3, it is rather difficult to estimate because it involves quite complicated calculations. From Fig. 6, for d = 0.002 m, the Gradient increase in the characteristic curve is faster compared to the cases of d = 0.005 m and 0.008 m. Let us examine the formulation of the (I-V) characteristics in Eq. (16). The value of I depends on the capacitance value C_{tot}, where a significant negative value of C_{tot} will result in a reasonably large I value. If we look at the C_{tot} formula in Eq. (14), then we can see the capacitance equation related to the values of d and k, namely in the equation section

$$\left[2\varepsilon_0 d\tan\left(\tfrac{1}{2}\theta\right)+a\varepsilon_0-ka\varepsilon_0\right]\ln\left|\frac{\frac{1}{2}ka\cot\left(\frac{1}{2}\theta\right)-d-\frac{1}{2}a\cot\left(\frac{1}{2}\theta\right)}{d+\frac{1}{2}a\cot\left(\frac{1}{2}\theta\right)}\right|$$

(20)

From Table 1, for the case d = 0.002 m, it has a larger k value when compared to d = 0.005 m and 0.008 m. From Eq. (20) for the value d = 0.002 m (small value) with a considerable k value will produce a significant C_{tot} value (but negative value), so that in the end it will produce a large electric current I (positive value) in Eq. (16) which causes the σ (SD) value to be significant in Eq. (18), thus reducing the level of accuracy between the analytical curve and the data points.

As shown in Fig. 7, the corona discharges are ordered from the most significant discharge flow to the smallest for $\theta = 30^0$, 45^0, and 60^0. This situation can occur because the sharper the angle of the active electrode, the greater the corona discharge will be.

The characteristic curve with the smallest SD value of 0.3352 (at variation $\theta = 60^0$ and d = 0.008 m) has an analytical curve slope following the research data in Fig. 6. In general, on the (I-V) characteristic curve (Fig. 6) with an explanation of the data in Table 1, we get the result that the higher the value of d, the lower the value of k, resulting in a minor distance deviation difference between the data points and analytical simulation curve, which ultimately produces the small average values of the t-test and SD at the case of furthest distance from d (0.008 m).

In this study, several differences were obtained in the research error values (t-test and SD) and the level of agreement between the data points and the analytical curve. Using variations of θ and d in Table 1, it turns out that the (I-V) characteristic curve produces a percentage of tangent point values relatively high on average. This situation indicates a relatively high level of agreement between the data points and the analytical curve derived from Eq. (16).

4. Conclusion

After going through the discussion chapter of the research results on the study of the calculation of the (I-V) characteristics of plasma discharges using the TBFA-P electrode construction model in air, we can obtain several conclusions as follows. Reviewing all research on the (I-V) characteristic curves involving variations in θ and d produces t-test error values below 0.05 and a high percentage of tangency points between the simulation curve and experimental data, indicating that the analytical formulation follows the research data. The corona discharge's (I-V) characteristic pattern can use a reduced capacitance model, which is much simpler than physical model calculations (using Maxwell's equations). The k factor, appearing as a corona current multiplier factor, calculated by Python GUI Programming (as a curve fitting), is a geometrically differentiating factor (because only the sharp tip of the active electrode produces a significant corona current discharge) with the conventional capacitance model. The results obtained for the case of the same angle θ apparently produce a tendency: the greater the distance d, the smaller the k value will be. This condition also affects the level of accuracy between the formulation of the analytical curve and the data points, namely that the greater the distance d, the smaller the difference in distance deviation (closer) between the analytical simulation curve and the data points.

Acknowledgment

This work was supported by non-tax revenue (PNBP), Diponegoro University, Semarang, Indonesia under contract No. 257-19/UN7.P4.3/PP/2019.

References

[1] S. Kim, and C. Kim, "Applications of Plasma-Activated Liquid in the Medical Field" Biomedic. 9(11), 1700, (2021).

[2] H. D. Stryczewska, and O. Boiko, "Applications of Plasma Produced with Electrical Discharges in Gases for Agriculture and Biomedicine" Appl. Sci., 12(9), 4405, (2022).

[3] A. K. Makar, "An Audit of Occurrence of Dust in Tokamak and Stability of Fusion Plasma" Plasma Fusi. Resear., 15, 1405019.1-1405019.8, (2020).

[4] Y-M. Lim, Y. He, J. Lee, J-H. Kim, K-H. Kim, and C-W. Chung, "Enhanced plasma generation in capacitively coupled plasma using a parallel inductor" Plasma Sour. Sci. Techn., 31(6), (2022).

[5] Y-X. Liu, W. Jiang, X-S. Li, W-Q. Lu, and Y-N. Wang, "An overview of diagnostic methods of low-pressure capacitively coupled plasmas" Thin Solid Films, 521, 141-145, (2012).

[6] Y. Guan, R. S. Vaddi, A. Aliseda, and I. Novosselov, "Analytical model of electrohydrodynamic flow in corona discharge" Phys. Plasmas, 25(8), 083507, (2018).

[7] M. Robinson, "Convective Heat Transfer at The Surface of A Corona Electrode" Int. J. Heat Mass Trans., 13, 263-274, (1970).

[8] M. Robinson, "Movement of Air in the Electric Wind of the Corona Discharge" Trans. Am. Inst. Elect. Eng., 80, 143-150, (1961).

[9] J. R. Bush, P. L. Feldman, and M. Robinson, "High Temperature, High Pressure Electrostatic Precipitation" J. Air Pollu. Contr. Assoc., 29(4), 365-371, (1979).

[10] M. Robinson, "The Corona Threshold for Coaxial Cylinders in Air at High Pressures" IEEE Trans. Power App. Syst., 86(2), 185-189, (1967).

[11] D. Halliday, R. Resnick, and J. Walker, "Fundamentals of Physics 10th ed." John Wiley & Sons, (2013).

[12] A. Y. Wardaya, Z. Muhlisin, J. E. Suseno, Q. M. B. Soesanto, M. Azam, E. Setiawati, and S. Hadi, "The electrode model of corona plasma discharge theory for current–voltage characteristics case in air" Euro. Phys. J. Appl. Phys., 97, 22, (2022).

[13] A. Y. Wardaya, Z. Muhlisin, J. E. Suseno, M. Nur, P. Triadyaksa, A. Khumaeni, E. A. Sarwoko, J. Windarta, and S. Hadi, "The Current-Voltage Characteristics for Electrode Geometry Model of Positive DC Corona Discharge in Air" Gazi Uni. J. Sci., 35, 1140-1150, (2022).

[14] J. Dobranszky, A. Bernath, and H. Z. Marton, "Characterisation of the plasma shape of the TIG welding arc" Int. J. Microst. Mater. Proper.,

3(1), 126-140, (2008).
[15] E. M. van Veldhuizen, and W. R. Rutgers, “Corona Discharges: Fundamental and Diagnostics” Frontiers in low temperature plasma diagnostics IV: papers. Rolduc Conf. Centre, 40-49, (2001).
[16] Y. Zheng, B. Zhang, and J. He, “Current-voltage characteristics of dc corona discharges in air between coaxial cylinders” Phys. Plasmas, 22, 023501-0235016, (2015).
[17] G. F. L. Ferreira, O. N. Oliveira Jr., and J. A. Giacometti, “Point-to-plane corona: Current-voltage characteristics for positive and negative polarity with evidence of an electronic component” J. Appl. Phys., 59, 3045-3049, (1986).
[18] A. Y. Wardaya, Z. Muhlisin, J. E. Suseno, C. Munajib, S. Hadi, H. Sugito, and J. Windarta, “Capacitance Calculation Model in Corona Discharge Case” Math. Model. Eng. Probl., 9(5), 1161-1171, (2022).
[19] A. D. Moore, “Mastering GUI Programming with Python: Develop impressive cross-platform GUI applications with PyQt” Packt Publishing, (2019).